PCCP

Accepted Manuscript

ROYAL SOCIETY OF CHEMISTRY

www.rsc.org/pccp

Physical Chemistry Chemical Physics
CREATED USING THE RSC LaTeX PCCP ARTICLE TEMPLATE – SEE www.rsc.org/electronicfiles FOR DETAILS
ARTICLE TYPE www. rsc.org/xxxxxx | XXXXXXXX

A Comparative Computational Study on the Hydrogen Adsorption on the Ag^+, Cu^+, Mg^{2+}, Cd^{2+}, and Zn^{2+} Cationic Sites in Zeolites†

Paweł Kozyra,[*a] **Witold Piskorz**[a]

Received Xth XXXXXXXXXX 20XX, Accepted Xth XXXXXXXXX 20XX
First published on the web Xth XXXXXXXXXX 200X
DOI: 10.1039/b000000x

In this article the interaction between H_2 and Ag^+, Cu^+, Mg^{2+}, Cd^{2+}, and Zn^{2+} cations in cluster models of several sizes has been studied computationally. Depending on the changes imposed by the adsorption process on H_2 molecule the activation can vary in wide range – from only slight weakening of H-H bond to complete dissociation of H_2 molecule. The NOCV (Natural Orbitals for Chemical Valence) analysis allowed for decomposition of the electron density distortion into contributions easier for interpretation. Three essential factors have been identified (*i*-*iii*). In the case of bare cation the main contribution is a donation from σ_{H_2} to the cation (*i*). When zeolite framework surrounding the cation is introduced, it hinders σ-donation and enhances π-backdonation from the cation to antibonding orbital of the molecule (*ii*). For Cu(I) and Ag(I) sites π-backdonation becomes dominant while for Mg(II), Cd(II), and Zn(II) cations the σ-donation, albeit diminished, still remains a dominant contribution. Calculation showed that the localization and coordination of the Zn(II) have crucial influence on its interaction with H_2. We identified a Zn^{2+} position for which H_2 molecule dissociates – here the interaction between H_2 and oxygen framework (*iii*) plays crucial role. Based on the calculations the mechanism of H_2 transformations has been proposed. Upon heterolytic dissociation of H_2 the Zn^0 moiety and two OH groups can be formed. Eventually, in two elementary steps H_2 molecule can be restored. In this case, the ability of the site to activate/dissociate hydrogen is caused by low coordination number of zinc cation and the geometry of the site which allows positively charged H_2 to interact with framework oxygen – it enhances formation of OH and $Z-O-(ZnH)^+$ groups.

1 Introduction

Hydrogen adsorption and activation are important for catalytic hydrogenation and other reactions involving hydrogen transfer, and, as such, are crucial for research concerning fuel cells or hydrogen storage,[1–3] to recall just a few processes. The zeolite cationic sites are known for activation of π-bonds[4–12] and also of σ-bonds, in, *i.e.,* H_2. Depending on the cationic site in MeMFI the adsorption energy and the H_2 activation extent, measured by stretching red-shift, can vary in a wide range – from only slight weakening of H-H bond to the dissociation of H_2 molecule. The MeMFI systems are also active in alkane/arene involving processes like dehydrogenation[13] and aromatization of light alkanes,[14–17] and also in alkylation processes.[18]

The low interaction energy (3 to 5 kcal/mol) between H_2 and the zeolitic sites (*e.g.*, Li^+, Na^+, K^+, Mg^{2+}, Ca^{2+}) drew attention of several scientific groups in the field of hydrogen storage.[19–29] However, hydrogen concentration in high-silica zeolites are much lower than the values acceptable for commercial use (*ca.* 6 % mass).

The aim of this article was to study the H-H activation properties of the sequence of cationic zeolite systems, and further study of the most active, which was found to be ZnMFI, and whose activity was also confirmed experimentally.[16,30] Besides Zn^{2+}, three other cations with d^{10} electron cofiguration, Ag^+, Cu^+, and Cd^{2+}, have been chosen for the case study while Mg^{2+}, a non-transition cation, was used as the reference. In spite of the same configuration of the valence shell, the cations behave/interact with hydrogen in different ways. Although hydrogen is unusually strongly activated by CuMFI, it does not dissociate.[27,31,32] The process of hydrogen activation by the cation sites was studied by means of the ETS-NOCV analysis and the energetic contributions were obtained – donation, backdonation, and covalent, constituted a novel "geometric" descriptor, Δr_{HH}^{NOCV}, which was further correlated to the geometric parameter, Δr_{HH} (see *Results and discussion* section).

† Electronic Supplementary Information (ESI) available: [details of any supplementary information available should be included here]. See DOI: 10.1039/b000000x/

[a] *ul. Ingardena 3, 30-060 Kraków, Poland. Fax: (++48) 126340515; Tel: (++48) 126632081; E-mail: kozyra@chemia.uj.edu.pl*
* Corresponding author

In this context the H-H bond activation resembles that of C-H; indeed, the ZnMFI catalyst is also active toward methane or other alkanes.[31,33–36] The mono-[37] and dinuclear[38,39] zinc sites were considered to be active towards hydrogen molecule. In the work of Kazansky *et al.*[40] the heterolytic nature of two-site H_2 dissociation into cationic $H^+ - O_{zeolite}$ and anionic $H^- - Zn(II)$ is emphasised.

Zinc cation can coordinate to zeolite framework at various sites. Calculation showed that localization and coordination of the cation have crucial influence on the interaction between the cation and H_2 and at some sites H_2 dissociates upon adsorption.[41] Even though the localisation of copper and zinc cations in the MFI framework is similar, the H_2 activation properties are different. Shubin *et al.*[42] have considered the site for which the barrier for hydrogen dissociation is 10.5 kcal/mol, however, the experimental data[43] shows that H_2 dissociate spontaneously. We have considered the zinc sites which are active in spontaneous dissociation of hydrogen. According to the results of Shubin *et al.* the hydrogen atom is labile and can migrate in the zeolite framework easily, however, in the raised temperature the hydrogen atom bound to Zn^{2+} ion can also migrate forming a second OH group.

In the present paper the mechanism for both spontaneous dissociation as well as for formation of Zn^0 and hydrogen desorption, being in good agreement with the model suggested by Oda[43], is proposed. Surprisingly, even though the redox potential is positive for Cu and negative for Zn, the activation of hydrogen molecule on Zn site is much deeper (eventually leads to H_2 dissociation) rather than on Cu site. The pivotal issue of this article was to elucidate this phenomenon and thus to complement the article of Oda *et al.*[43] by qualitative justification of the hydrogen transformation in ZnMFI.

Methodology

Models

As models of cationic sites we used bare cations of copper(I), silver(I), magnesium(II), cadmium(II), and zinc(II) as well as these cations coordinated to $[Al(OH_4)]^-$ anion (T1), or M7 frameworks, the latter composed of seven silica tetrahedra. Hydrogen molecule is bound side-on both with bare cations and with cation sites (see Fig. 1). For divalent exchanged cations the T8 and T11 (see Fig. 1 in the Supporting Information to recall the naming convention) positions of Al atoms was used, labelled S2 by Oda *et al.*,[43] whereas for monovalent cations one Al was introduced in the T7 position so that all the models are electrostatically neutral. The S2 model was chosen based on the conclusion[43] of higher energy barrier for H-H dissociation for S3 (attributed to the longer distance between Al atoms in S3 model compared to S2, which makes dissociation a less concerted and thus more energetically hindered process) and also the larger discrepancies between calculated and experimental wavenumbers. The S1 and S4 models were discriminated due to the closer distance between two Al atoms which causes excessive charge build-up repulsing the divalent zinc ion.

The hydrogen atoms of the terminating OH groups were placed along the O-T' bond (where T' is the next T site, replaced by H atom in this model) but at the distances of 0.9666 Å and 0.9628 Å in silicon or aluminium T site, respectively. The positions of these hydrogen atoms have been fixed to preserve the structure of the zeolite framework.

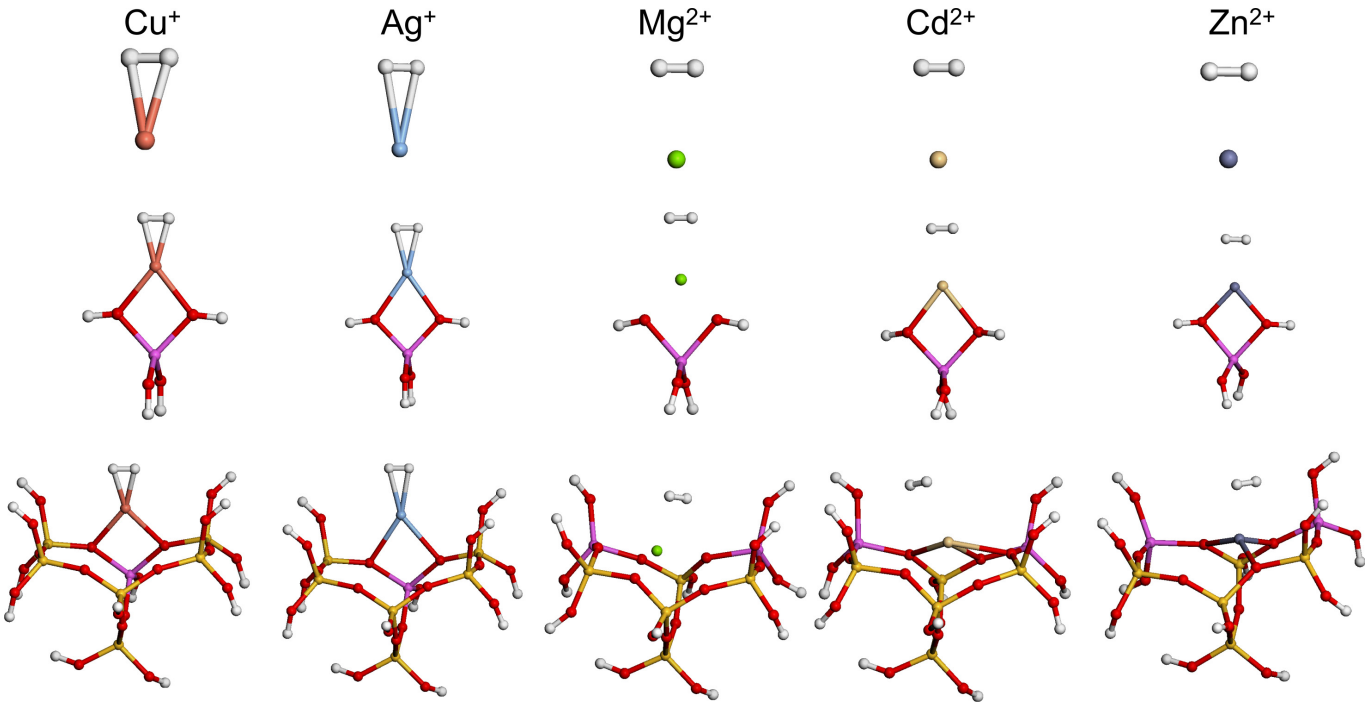

Fig. 1 Qualitative view of the discussed models.

Computational details

Geometry optimization and vibrational analysis have been done with Turbomole package on the DFT B3LYP level of theory with def2-TZVP basis set.[44]

Even though the inclusion of dispersion interactions can improve the total SCF energy values it is not necessarily the case when the relative energies (*i.e.*, for barriers) are studied. In fact, Lochan *et al.*[45] discuss the importance of the contributions to the total binding energies (electrostatic, dispersion, and orbital interactions) for the H-storage materials like MOFs, dehydrated Prussian blue analogues or others. They emphasise that in the studied systems it is the orbital energy that plays the decisive role in the selection of the elementary steps. To verify the applicability of that statement in the system studied in this article the DFT+D[46] computations were redone and it was concluded that even though the total ESCF indeed changed significantly (a few tens of kcal/mol), the binding and barrier energies changed only by $\leqslant 4$ and $\leqslant 0.4$ kcal/mol, respectively, upon inclusion of the dispersion forces, even though the full geometry re-optimisation was performed. However, to be able to compare our results to those obtained by Oda the non-D energies are presented hereafter. The set of DFT+D *vs.* DFT energies for the first 7 structures (5 minima and two TS) are summarised in the ESI.

The difference between electron density of the composed system and the sum of densities of non-interacting fragments in the geometries of the complex (deformation density $\Delta\rho$) is represented by deformation density matrix $\Delta\mathbf{P}$. The Natural Orbitals for Chemical Valence (NOCV) are defined as the eigenvectors, ψ_i (expressed in the orthogonalized basis set of N fragment molecular orbitals ϕ_j), diagonalizing deformation density matrix, $\Delta\mathbf{P}$: $\Delta\mathbf{P}\,\mathbf{C}_i = \lambda_i\,\mathbf{C}_i$, where $\mathbf{C}_i$ is a vector of the coefficients in the basis ϕ_j, and λ_i is the i-th eigenvalue, a descriptor for the number of electrons transferred along selected channel. Deformation density can be expressed as a sum of pairs of ordered complementary orbitals (λ_{-k}, λ_k) corresponding to eigenvalues equal to the absolute value, but with opposite signs[47–50] defining independent density transfer channels ($\Delta\rho_k$):

$$\Delta\rho(r) = \sum_{k=1}^{N/2} \lambda_k \left[-\psi_{-k}^2(r) + \psi_k^2(r)\right] = \sum_{k=1}^{N/2} \Delta\rho_k(r) \tag{1}$$

The NOCV decomposition of the differential density given by Eq. 1 may be linked to Ziegler-Rauk energy decomposition approach (Extended-Transition-State, ETS).[51] Total interaction energy between two fragments may be decomposed, according to ETS, into the following terms: $\Delta E_{\text{total}} = \Delta E_{\text{dist}} + \Delta E_{\text{Pauli}} + \Delta E_{\text{elstat}} + \Delta E_{\text{orb}}$. The distortion energy, ΔE_{dist}, is the energy needed

to change the geometry of non-interacting fragments to that in the complex. The Pauli term, $\Delta E_{\mathrm{Pauli}}$, is associated with repulsion of closed shells of fragments. The electrostatic component, $\Delta E_{\mathrm{elstat}}$, is an energy of interaction between electron densities on both fragments (promolecules). The orbital term, ΔE_{orb}, is an orbital interaction energy of the fragments, including inter- and intrafragment polarization. By applying ETS-NOCV method the last term (ΔE_{orb}), describing the part of adsorption energy due to direct electronic interactions, was decomposed into contributions corresponding to independent electron transfer channels spanning deformation electron density. The ETS-NOCV analysis has been performed with partition of the system into two fragments: the hydrogen molecule, and the rest of the system, a free or embedded cation.

Additionally, for zinc site the conceivable paths of hydrogen transformation were analysed. The optimized zinc sites, however, turned out to be inactive toward hydrogen dissociation hence the dissociation product structure ($Z-O-(ZnH)^+$ and $Z-OH$ groups) was optimised instead. After having moved H atoms together the resultant H_2 departed the system leaving the Zn^{2+} cation in the position where it was active in H_2 decomposition.

Since it was experimentally showed that at raised temperature the $Z-O-(ZnH)^+$ and $Z-OH$ groups transform into two $Z-OH$ groups and Zn^0, and at even higher temperature the restoration of H_2 is observed,[43] the direct process of H-H association was studied by bringing H atoms (of $Z-OH$ groups) together but in such scheme the H_2 molecule was not restored but rather one of H atoms formed a bond with Zn^0. The different scheme, commenced by the restoration of $Z-O-(ZnH)^+$ and $Z-OH$ groups, lead, however, to forming the H_2 molecule. It can be rationalised by the opposite partial charges accumulated on H atoms. It was not the case for the previous mechanism, where both H atoms in OH groups were positively charged, and hence the restoration of H_2 was not feasible.

The forming/breaking bond in the elementary steps was scanned by means of the routine LST/QST (own extension to the QMPot code[52,53]) procedure and the resulting TS guess was optimised (Powell update of the Hessian) with constrained proper Hessian curvature. The optimised TS was eventually verified by the harmonic vibrational analysis.

Results and discussion

Hydrogen activation on bare cations, and T1 and M7 sites

The values of H-H bond elongation and stretching frequency red-shift, with respect to the gas phase hydrogen molecule, are given in Fig. 1 as the measures of the extent of activation. Bond length is related to calculated value for free molecule (0.744 Å, while experimental values is 0.741 Å[54]). The red-shifts are calculated as the differences between the calculated harmonic frequency for H_2 of 4418 cm^{-1}, close to the experimental harmonic frequency of 4401 cm^{-1}.[54] Experimental frequency value for para-H_2 (4161 cm^{-1}) is taken as the reference for experimental shifts.[55] Hydrogen molecule adsorbed on Brønsted acid or sodium sites exhibit red-shift of *ca.* 60 cm^{-1} [37,56] while the values for hydrogen interacting with free silver and copper cations are 8-10 times higher.[37,57]

Table 1 The measures of H-H bond activation – Δr_{HH}, $\Delta\nu$, and ΔE_{total}.

Model label	Model	Coord number	r_{MH} /Å	Δr_{HH} /pm	$\Delta\nu$ /cm^{-1}	ΔE_{total} /kcal·mol^{-1}
a	$[AgH_2]^+$	0	2.04	3.1	−442	−10.0
b	$[(T1)AgH_2]^0$	2	1.77	5.1	−769	−11.3
c	$[(M7)AgH_2]^0$	2	1.93	3.6	−506	−6.4
d	$[CuH_2]^+$	0	1.77	4.2	−600	−22.6
e	$[(T1)CuH_2]^0$	2	1.61	7.7	−1133	−23.8
f	$[(M7)CuH_2]^0$	2	1.65	6.1	−502	−13.9
g	$[MgH_2]^{2+}$	0	2.04	3.7	−484	−24.6
h	$[(T1)MgH_2]^+$	2	2.12	1.5	−197	−10.2
i	$[(M7)MgH_2]^+$	2	2.03	1.1	−149	−4.1
j	$[CdH_2]^{2+}$	0	2.14	3.2	−407	−26.2
k	$[(T1)CdH_2]^+$	2	2.10	3.0	−421	−11.5
l	$[(M7)CdH_2]^+$	3	2.29, 2.44	2.2	−350	−4.9
m	$[ZnH_2]^{2+}$	0	1.88	7.8	−967	−44.1
n	$[(T1)ZnH_2]^+$	2	1.89	3.3	−454	−16.7
o	$[(M7)ZnH_2]^+$	4	2.14	1.3	−182	−3.6
p	$[(M7)ZnH_2]^0$	3	2.03, 2.14	2.5	−373	−4.5

Both Δr_{HH} and $\Delta\nu_{HH}$ vary significantly among the hydrogen molecules interacting with discussed cations (Table 1). Calculated red-shifts and H-H bond elongations are well correlated (Fig. 2). The slope of linear fit equals to -132 ± 5 cm$^{-1}\cdot$pm^{-1}. Experimental wavenumbers are easier to measure than bond length thus the dependence of $\Delta\nu_{HH}$ *vs.* Δr_{HH} allows for a quick estimation of the calculated hydrogen activation measure in case where IR data are available. It is especially useful for evaluating large models where vibrational analysis becomes prohibitively time consuming. It could also be potentially used for estimation of CO wavenumber as for some acidic and hard cationic zeolite sites the red-shift for H_2 is a doubled value for CO: $\Delta\nu_{HH} \approx 2\Delta\nu_{CO}$.[55,58]

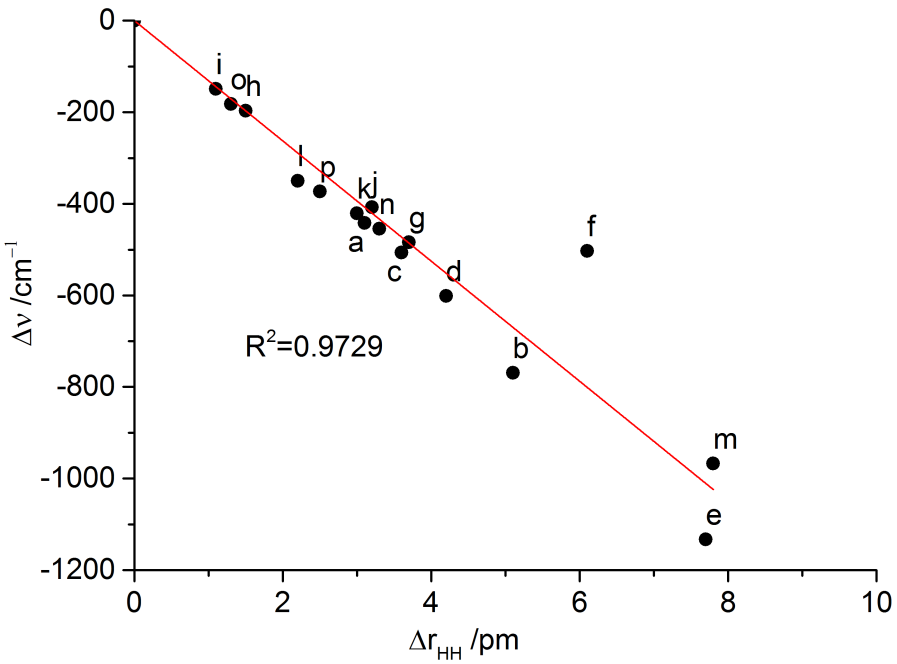

Fig. 2 Correlation between H-H bond elongation (Δr_{HH}) and IR red-shift ($\Delta \nu_{HH}$) cationic MFI sites. Labelling refers to Table 1.

The IR red-shift of H-H bond resulting from the interaction between hydrogen molecule and studied cation sites are in relatively wide range – from -149 cm^{-1} for magnesium site to -1133 cm^{-1} for copper site. Comparing the activation effect for bare cations and those surrounded by zeolite framework it can be concluded that for Ag(I) and Cu(I) the zeolite framework enhances the activation while for Mg(II), Cd(II), and Zn(II) is conversely. Calculated interaction energy (ΔE_{total}) is a measure of the strength of the hydrogen molecule bonding. However, it does not refer directly to the activation process. Indeed, for Mg(II), Cd(II), and Zn(II) the stronger interaction leads to the more efficient activation but it does not hold always. Contrary to ΔE_{total}, the orbital interaction energy of the systems, ΔE_{orb}, is well correlated with elongation of H-H bond (see Fig. 2). It implies that the activation is mainly determined by populating or depopulating the hydrogen molecule orbitals. It has also been previously stated[45] that in the case of hydrogen the orbital interaction energy, rather than electrostatic or dispersion contributions, is crucial for reproducing the substantial part of energy of interaction with host materials. In the copper containing zeolites some Cu^{2+} cations undergo autoreduction forming Cu^{+} cations while the rest of them remain in the original oxidation state and both constitute adsorption centres for hydrogen. For that reason, even though the Cu^{2+} cation, having d^9 configuration, is the open-shell system, contrary to those discussed in this article, we have performed analogous computation (see SI). For the Cu^{2+} cation, despite it having unpaired electron, the spin density does not change upon interaction with hydrogen molecule and this interaction resembles that for Mg(II), Cd(II), and Zn(II).

Table 2 Elongation of H-H bond (Δr_{HH}), orbital interaction energy (ΔE_{orb}), its contributions: σ-donation ($\Delta E_{\mathrm{orb}}^{\mathrm{don}}$), covalent component ($\Delta E_{\mathrm{orb}}^{\mathrm{coval}}$), π-backdonation ($\Delta E_{\mathrm{orb}}^{\mathrm{bdon}}$), and respective NOCV charge transfer estimates (λ^i). Empty cells denote negligible values.

Model	Coordinate number	Δr_{HH}/ pm	ΔE_{orb}/ kcal · mol^{-1}	σ-donation		Covalent component		π-backdonation	
				$\Delta E_{\mathrm{orb}}^{\mathrm{don}}$	λ^{don}	$\Delta E_{\mathrm{orb}}^{\mathrm{coval}}$	λ^{coval}	$\Delta E_{\mathrm{orb}}^{\mathrm{bdon}}$	λ^{bdon}
$[AgH_2]^+$	0	3.1	−15.3	−10.7	0.27	−2.7	0.11	−1.4	0.09
$[(T1)AgH_2]^0$	2	5.1	−29.9	−8.7	0.25	−8.6	0.18	−10.8	0.28
$[(M7)AgH_2]^0$	2	3.6	−15.5	−5.6	0.20	−5.1	0.15	−3.8	0.16
$[CuH_2]^+$	0	4.2	−27.3	−16.0	0.36	−7.2	0.19	−3.7	0.16
$[(T1)CuH_2]^0$	2	7.7	−37.2	−11.4	0.29	−9.9	0.21	−14.6	0.33
$[(M7)CuH_2]^0$	2	6.1	−28.8	−9.6	0.26	−8.7	0.19	−10.0	0.27
$[MgH_2]^{2+}$	0	3.7	−25.7	−25.6	0.37				
$[(T1)MgH_2]^+$	2	1.5	−11.2	−9.8	0.23				
$[(M7)MgH_2]^+$	2	1.1	−7.4	−6.1	0.18				
$[CdH_2]^{2+}$	0	3.2	−28.4	−27.4	0.42				
$[(T1)CdH_2]^+$	2	3.0	−11.2	−11.6	0.29				
$[(M7)CdH_2]^+$	3	2.2	−11.6	−10.4	0.26				
$[ZnH_2]^{2+}$	0	7.8	−46.9	−44.4	0.52	−4.0	0.05		
$[(T1)ZnH_2]^+$	2	3.3	−21.9	−15.6 −1.0*	0.33 0.08*			−5.3	0.08
$[(M7)ZnH_2]^0$	3	2.5	−15.7			−12.7#	0.30		

*– σ-backdonation

– with admixture of interaction between framework oxygen and H_2 molecule, see Fig. 6.

Much more detailed information on the interaction between H_2 and cation sites is delivered by the NOCV analysis. Using it the deformation density ($\Delta\rho$) is decomposed into a few contributions, $\Delta\rho_k$, which are easier for interpretation. The eigenvalues λ^i estimate the number of electrons transferred in the channels $\Delta\rho_k$. Moreover, the ETS-NOCV analysis delivers components of orbital interaction energy, $\Delta E_{\mathrm{orb}}^i$, relevant for electron density transfer channels $\Delta\rho_k$. These values give the information on the importance of each contribution to the deformation density. In all cases the significant contribution can be attributed to one of three channels: (*i*) donation from σ(H-H) to s orbital of the cation ($\Delta E_{\mathrm{orb}}^{\mathrm{don}}$), (*ii*) polarization toward the bonding region (donation to bonding H_2-M space with depopulation of σ_{H_2} and d_{z^2} orbitals), $\Delta E_{\mathrm{orb}}^{\mathrm{coval}}$, (*iii*) backdonation from d_π orbitals to $\sigma_{H_2}^*$ antibonding orbital, $\Delta E_{\mathrm{orb}}^{\mathrm{bdon}}$. All the contribution weaken the H-H bond and the second term, (*ii*), is also responsible for valence bonding between the hydrogen and the site. The (*i*) and (*ii*) contributions represent depopulation of the bonding orbitals while the (*iii*) contribution represents population of antibonding orbitals. The Analogous analysis for Cu^+ and Na^+ has been done by X. Solans-Monfort *et al.* by selectively deleting fragment virtual orbitals.[26] The authors also report the effect of favouring the charge transfer from $Cu^+(3d_\pi)$ orbital to the $H_2(\sigma^*)$. However, the NOCV method reveals even stronger influence of zeolite on backdonation. Thus in the next step we focused on the semi-quantitative analysis of the impact of each contribution to orbital interaction energy on hydrogen activation.

Having ΔE_{orb} decomposed, it is possible to determine the importance of particular contribution to hydrogen activation. The following equation has been optimized to reproduce calculated elongation of H-H bond:

$$\Delta r_{\mathrm{HH}}^{\mathrm{NOCV}} = c\left[\alpha\cdot\Delta E_{\mathrm{orb}}^{\mathrm{bdon}} + (1-\alpha)\left(\Delta E_{\mathrm{orb}}^{\mathrm{don}} + \Delta E_{\mathrm{orb}}^{\mathrm{coval}}\right)\right] \quad (2)$$

The contributions to orbital interaction energy, taken with optimized coefficients c and α, reproduced calculated H-H bond elongation well (Fig. 3). The coefficient $\alpha = 0.59$ indicates that backdonation processes have stronger impact on the adsorbed hydrogen molecule than those connected with depopulation of bonding orbitals ($1-\alpha = 0.41$) — the ratio between the respective values is approximately like 3 to 2. Despite the fact that the contributions to orbital interaction energy vary in a wide range (often some of them are absent), the linear dependency is preserved what confirms that orbital interaction is an important factor in the process of the hydrogen molecule activation. It can be also inferred that the α coefficient is relatively universal (at least for a given molecule).

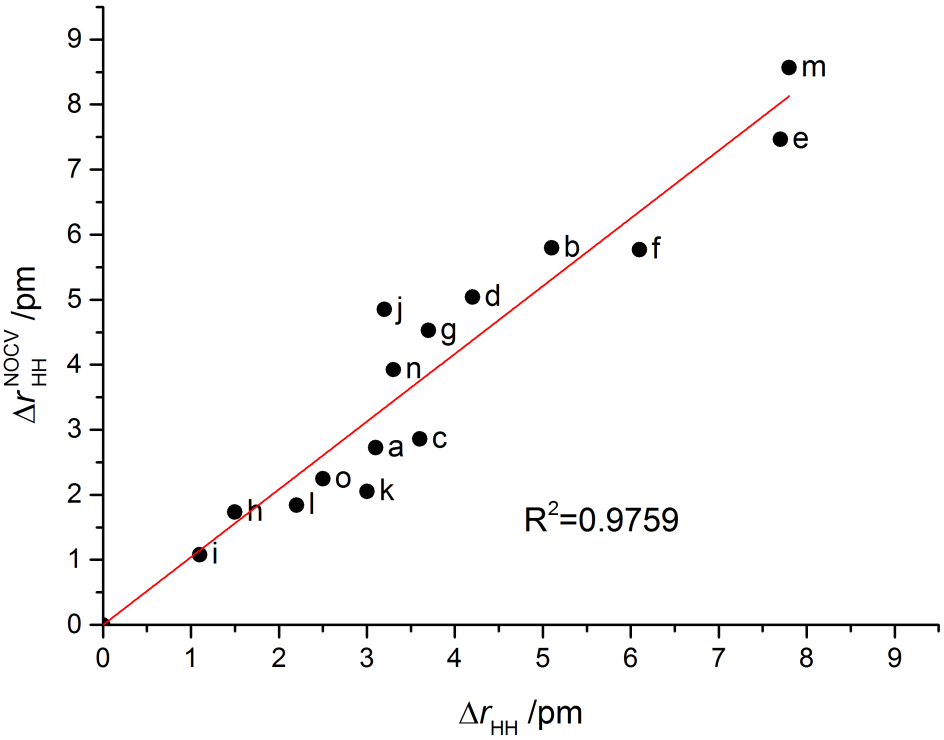

Fig. 3 H-H bond elongation calculated from contributions to orbital interaction energy (Δr_{HH}^{NOCV}) *vs.* calculated wave numbers (Δr). Labelling refers to 1.

The influence of the zeolite oxygen atoms can be elucidated from the results obtained for the systems with or without zeolite framework. When the cation is surrounded by the zeolite framework, the latter opposes σ-donation and enhances π-backdonation from the cation to antibonding orbital of the molecule. It holds for all cases studied and is apparently the result of interaction between the cations and free electron pairs of framework oxygen atoms. The less positively charged cations have lower ability to accept electrons while they are more efficient donors. Although cations are partially neutralized, only some of them exhibit significant ability as π-donors. These are Cu(I) and Ag(I) sites for which π-backdonation becomes dominating (see Fig. 4), while for Mg(II), Cd(II) and Zn(II) σ-donation, although diminished, still remains a dominant contribution (Fig. 5). Depending on the cation, for symmetric site-on adsorption, one of the channels determines the activation – either π-backdonation or σ-donation.

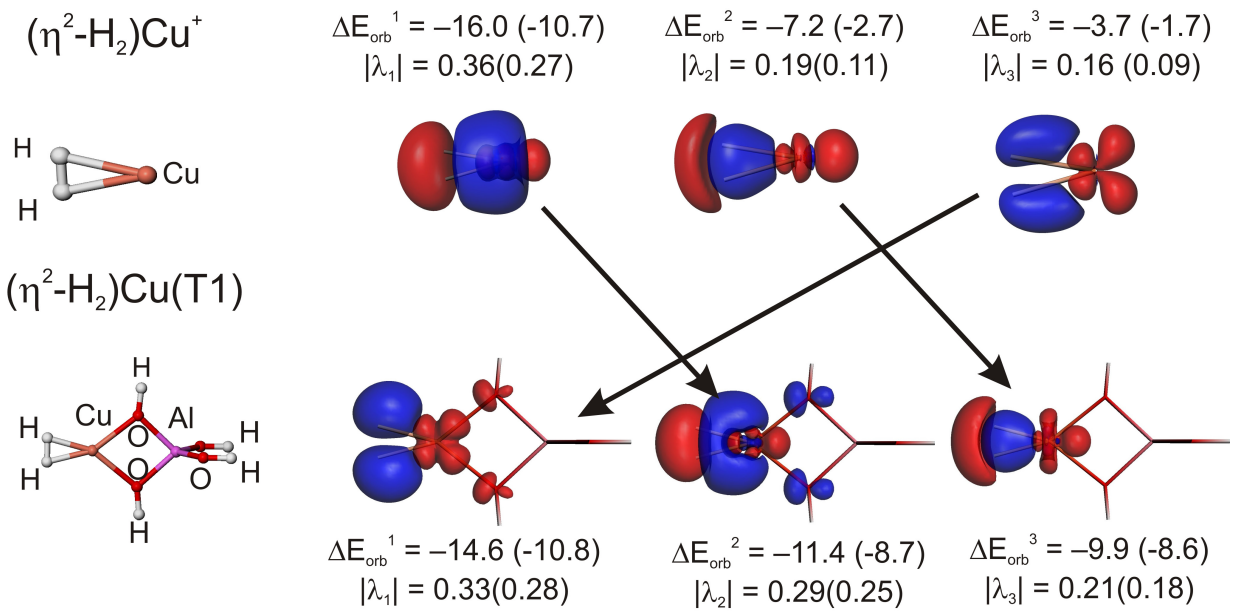

Fig. 4 Contribution to deformation electron density for $[(T1)CuH_2]^0$ together with the corresponding orbital interaction energy contributions (ΔE^i_{orb}/kcal · mol^{-1}) and NOCV charge transfer estimates (λ_i). Data in parentheses for Ag^+, red (light grey) – density outflow, blue (dark grey) – density inflow (contour value 0.001 a.u., colour figures on-line).

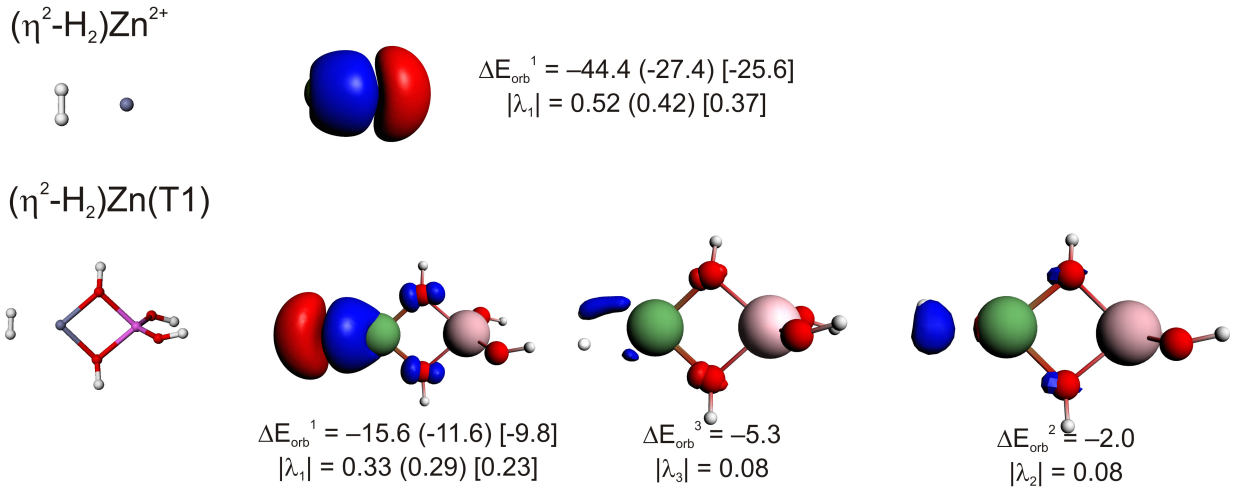

Fig. 5 Contribution to deformation electron density for $[(T1)ZnH_2]^+$ together with the corresponding orbital interaction energy contributions (ΔE^i_{orb}/kcal · mol^{-1}) and NOCV charge transfer estimates (λ_i). Data in parentheses for Cd^{2+}, data in square brackets for Mg^{2+}, red (light grey) – density outflow, blue (dark grey) – density inflow (contour value 0.001 a.u., colour figures on-line).

In the models described above the zeolite framework binds the cations, delivers electrons to them, but does not interact with hydrogen molecule directly. Expanding the model to M7 the modes of adsorption remain the same for all systems but $[(M7)ZnH_2]^0$ and $[(M7)CdH_2]^0$, in which hydrogen molecule is not adsorbed symmetrically – the distance between the cation and hydrogen atoms are different. It is caused by the interaction between positively charged hydrogen and framework oxygen atoms in its vicinity what is visible in the Fig. 6. Electron density flows mainly from σ-orbital of H_2 molecule to bonding area between Zn^{2+} cation and the adsorbed molecule. Moreover, framework oxygen donates electrons from its lone pair. As a

result, the H_2 molecule is polarized and it is reflected in the second contribution to deformation density. The H_2 molecule is not dissociated and H atoms are not equivalent – one is in its half way to form Zn-H bond and the second is to form the OH group. The whole system adapts a transition state-like geometry.

Even though the M7 model brought fruitful observation on how hydrogen interacts with the zinc site, further extension of the model by additional two tetrahedra was necessary (M9 model) having realised that the crucial oxygen atom is linked to hydrogen terminating model.

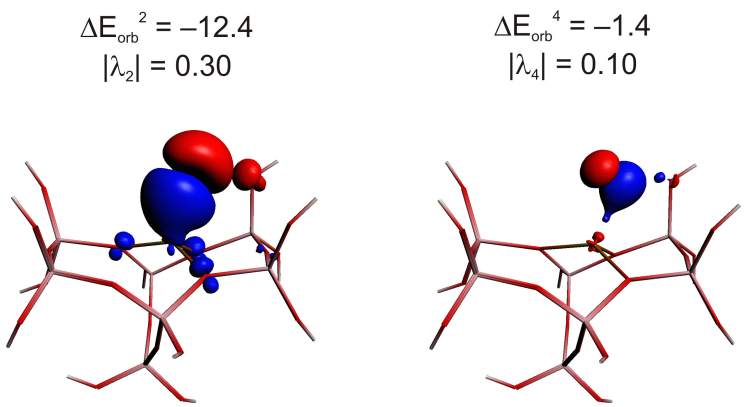

Fig. 6 Contribution to deformation electron density for $[(M7)ZnH_2]^0$ together with the corresponding orbital interaction energy contributions (ΔE^i_{orb}/kcal · mol^{-1}) and NOCV charge transfer estimates (λ_i). Red (light grey) – density outflow, blue (dark grey) – density inflow (contour value 0.001 a.u., colour figures on-line).

Transformation of hydrogen on Zn^{2+} zeolite sites

Concerning zinc sites several models of the certain range of size and for 0 to 2 aluminium atoms (Fig. 7) were studied. Even in the same model zinc cation can form differently coordinated sites in the zeolite framework. In the Table 3 the models for zinc site are listed with relative energy, elongation of H-H bond, and population analysis.

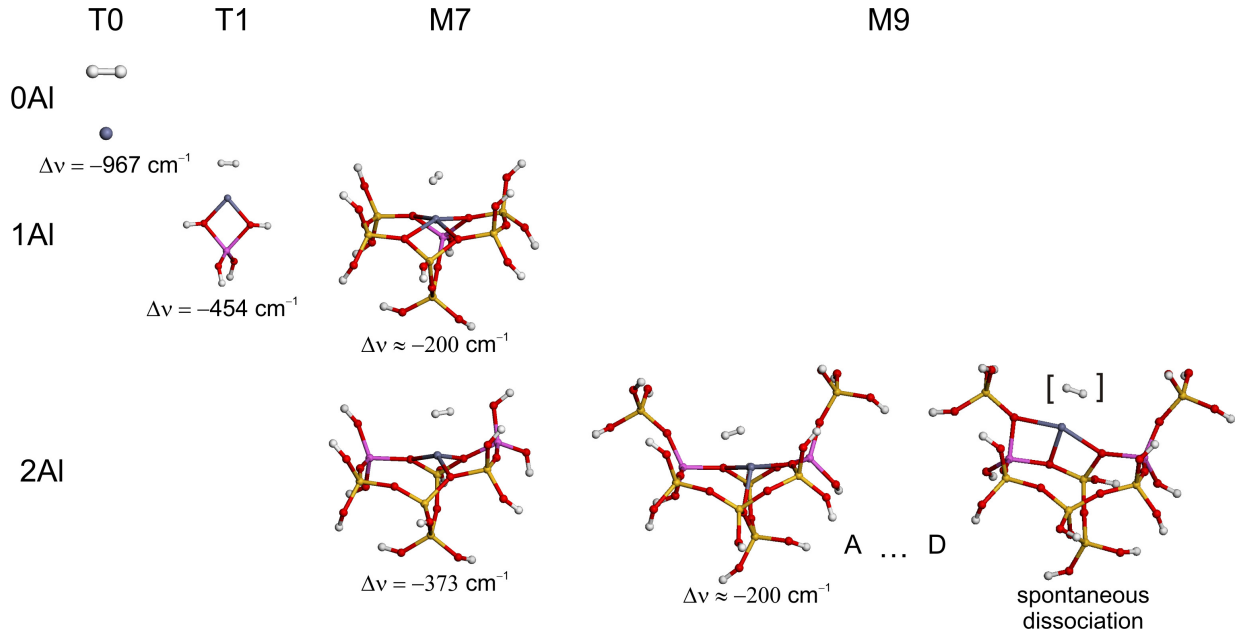

Fig. 7 IR peak shifts for studied models.

Table 3 Adsorption energies (ΔE_{ads}), H-H bond elongation (Δr_{HH}) and Mulliken population analysis for hydrogen on Zn site models

Model	ΔE_{ads} / (kcal · mol^{-1})	r_{MH}/Å	r_{MO}/Å	Δr_{HH} / pm	$q_{Zn}/\|e\|$	$q_{H_A}/\|e\|$	$q_{H_B}/\|e\|$	$q_Z/\|e\|$
$[ZnH_2]^{2+}$	−44.1	1.88	–	7.8	1.50	0.25	0.25	—
$[(T1)ZnH_2]^+$	−16.7	1.89	1.87; 1.87	3.3	0.75	0.15	0.15	−0.05
$[(M7)ZnH_2]^+$	−3.6	2.14	2.06; 2.06; 2.19; 2.23	1.3	0.80	0.08	0.06	+0.06
$[(M7)ZnH_2]^0$	−4.5	2.03; 2.14	2.02; 2.07; 2.09	2.5	0.80	0.03	0.14	−0.97
$[(M9)ZnH_2]$ A	−4.0	2.12	2.03; 2.05; 2.14; 2.18	1.4	0.86	0.08	0.05	−0.99
$[(M9)ZnH_2]$ B	−5.1	2.12	2.03; 2.03; 2.15; 2.18	1.4	0.91	0.09	0.04	−0.94
$[(M9)ZnH_2]$ C	−3.3	2.12	2.07; 2.12; 2.13; 2.21	1.4	0.88	0.12	0.04	−1.04
$[(M9)ZnH_2]$ D *	−41.4	1.53	1.90	dissoc.	0.46	0.31	−0.05	−0.72

* – structure labelled as **2** in the further part of the text

Among bare cations, zinc activates the H-H bond to the largest extent, $\Delta\nu = -967$ cm^{-1}. Indeed, the contribution to orbital interaction energy attributed to σ-donation is -44 kcal · mol^{-1} – the zinc cation has the greatest acceptor properties among analysed ones and the Mulliken population analysis indicates its withdrawal of 0.5 e from hydrogen molecule. Upon coordination by alumina tetrahedron (T1) the σ-donation channel is diminished and also hydrogen activation is weaker. The Mulliken analysis shows that in this case 0.3 e is transferred from hydrogen molecule to zinc site which is additionally partly neutralised by T1 – it gains a total of 0.95 e. For M7 cluster with one aluminium atom the zinc cation is four-fold coordinated and the red-shift is as low as -182 cm^{-1} and only 0.14 |e| is taken from hydrogen. The extent of the activation is strongly correlated with coordination number as for M7 cluster with two aluminium atoms zinc cation is coordinated to three oxygen atoms and the red-shift falls between those for two-fold and four-fold coordinated zinc cations. For M7 cluster with two aluminium atoms the hydrogens are in different distance from zinc cation presenting the distorted side-on mode of adsorption. As the result, the hydrogen molecule is polarized – one H atom has charge $q/|e| = +0.03$ while the other has $q/|e| = +0.14$ – see also Fig. 6. It is caused by the interaction between positively charged hydrogen and framework oxygen atom. This oxygen atom is linked to terminating hydrogen of the M7 cluster and hence is poorly represented in the relatively small M7 structure. Thus the system has been extended by another two tetrahedra, as mentioned above, yielding the larger cluster, M9, for which two stable zinc cation localizations were found. On the more stable site in M9, not active toward hydrogen dissociation, three modes of adsorption were found (Fig. 8). The analogous modes, with geometries and red-shifts very close to ours, have been studied by Shubin *et al.*,[42] who found the dissociation and diffusion pathway with energy barriers of ~ 10 kcal · mol^{-1}, relatively very small comparing to the hydrogen dissociation energy of 104 kcal · mol^{-1}.[54]

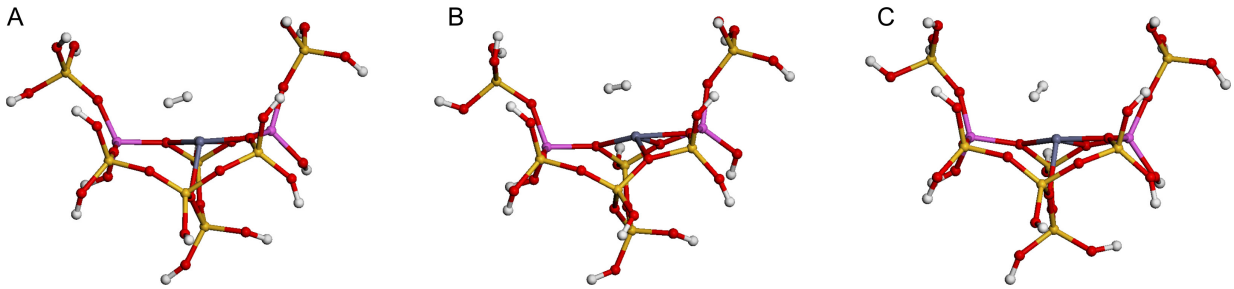

Fig. 8 Modes of H_2 adsorption on ZnM9 site.

In all these modes the H-H bond is elongated by only 1.4 pm and the red-shifts remain in the range of -196 cm^{-1} to

-201 cm^{-1} thus only slight activation is observed. However, the H_2 molecule dissociates spontaneously on the second type of zinc site. According to EXAFS experiment,[43] zinc cation in such active site is three-fold coordinated. On the basis of calculations, we found two active, almost equivalent, zinc positions – structures **1** and **8** presented in Fig. 9. Calculations confirmed the activity of these zinc sites toward spontaneous hydrogen dissociation. The mechanism of H_2 transformation has been proposed in Fig. 9. The IR measurements identified absorption bands corresponding to $(ZnH)^+$ stretching mode at 1933 cm^{-1} and the OH group band at 3615 cm^{-1}.[43] The structure **2** shows the product of hydrogen molecule dissociation upon adsorption on the site **1**. Vibrational analysis for the former structure gives the wavenumbers of 1907 cm^{-1} and 3570 cm^{-1} which reasonably match the experimental ones and also the computational results of Oda *et al.* (*op. cit.*), 1922 cm^{-1} and 3656 cm^{-1}, respectively. The Mulliken population analysis gives the charge $q/|e| = +0.31$ for one hydrogen, the value typical for OH groups, while for the other $q/|e| = -0.05$, what indicates the slight hydride type of that hydrogen.

Upon heterolytic dissociation of H_2 the Zn^0 moiety can be formed together with two OH groups (structure **4**). Calculated wavenumbers for these OH groups are equal to 3287 cm^{-1} and 3580 cm^{-1}. It is observed experimentally as increasing of IR band intensity at 3615 cm^{-1} and also by DRIFT UV spectroscopy (absorption peaks in the range of 42000 cm^{-1} and 47000 cm^{-1} are assigned to Zn^0).[43] The Mulliken charges are consistent with this interpretation yielding $q/|e| = +0.01$ for Zn, which is indeed at zero valence state, and $q/|e| = +0.26$ and $q/|e| = +0.32$ for hydrogen atoms forming OH groups. From the experiment it is known that at 600 °C hydrogen desorbs and zinc site is restored. According to our calculation this process runs in two elementary steps. The H atoms (of OH groups), approaching each other, do not form a molecule as they are both positively charged — one of them rather tends to form the Zn-H bond — so the first step of hydrogen desorption is again the formation of OH group and $Z-O-(ZnH)^+$. Depending on which OH bond is cleaved the reaction can proceed forward (to structure **6**) or backward (to structure **2**). As the structure **6** is similar to the structure **2**, the corresponding wavenumbers are close to each other, namely 1940 cm^{-1} for ZnH bond and 3692 cm^{-1} for OH group, respectively. For the structure **6** hydrogen atom bound to zinc ion has slightly negative Mulliken charge ($q/|e| = -0.02$), while the other is positively charged ($q/|e| = +0.34$). In the last step, leading to **8**, the H_2 molecule is restored. Obviously, the structure **8** is also active in hydrogen dissociation. According to computational results, there is virtually no barrier between structure **8** and structure **6** (upper bound of 0.5 kcal $\cdot$ mol^{-1}). Thus the hydrogen adsorption on the site **8** can lead to structure **6** or can proceed through the analogous, "mirrored", steps according to the path presented in Fig. 10.

Table 4 Energy changes between given elementary step and the first one (ΔE, 3rd column) or between given elementary step and the previous step ($\Delta E'$, 4th column). The energies in 4th column are: E_{SCF}; $\Delta G^{\ominus}(200\,°C)$; $\Delta G^{\ominus}(400\,°C)$; $\Delta G^{\ominus}(600\,°C)$, respectively.

Structure	Label, n	$\Delta E = E_n - E_1$ /(kcal $\cdot$ mol^{-1})	$\Delta E' = E_n - E_{n-1}$ /(kcal $\cdot$ mol^{-1})
[(M9)Zn]* + H_2	**1**	0	—
[(M9)ZnH_2]	**2**	−41.4	−41.4 ; −22.3 ; −15.6 ; −9.1
$TS_{2,4}$	**3**	−6.5	35.0 ; 36.0 ; 39.1 ; 42.4
[(M9)ZnHH]	**4**	−14.2	−7.8 ; −7.4 ; −10.0 ; −12.3
$TS_{4,6}$	**5**	5.8	20.1 ; 17.9 ; 17.6 ; 17.3
[(M9)HZnH]	**6**	−48.1	−53.9 ; −53.1 ; −53.1 ; −53.0
$TS_{6,8}$	**7**	−2.0	46.1 ; 30.0 ; 24.3 ; 18.1 *
[(M9)Zn]* + H_2	**8**	−2.5	**

* – $E_8 - E_6$; ** – negligible value; see text

The energy and the wavenumbers calculated for the structures **9**, **10**, **11** are very close to analogous structures **2**, **4**, **6**. For the structure **9** the wavenumbers for Zn-H and O-H bond are 1905 cm^{-1} and 3613 cm^{-1}, respectively. The wavenumbers for OH groups in the structure **10** are 3472 cm^{-1} and 3678 cm^{-1}. Moreover, the Mulliken population analysis for structures **9**, **10**, **11** also gives the values strictly resembling those for structures **2**, **4**, **6** – see Table 5. At the end of the transformation the structure **1** is formed – the cycle of hydrogen transformation is closed and the zinc site is restored. However, in the process of adsorption and desorption of hydrogen, zinc can get displaced (**1** $\rightarrow$ **8** or **8** $\rightarrow$ **1**) or return to the same position (**1** $\rightarrow$ **2** $\rightarrow$ **4** $\rightarrow$ **2** $\rightarrow$ **1** or **8** $\rightarrow$ **9** $\rightarrow$ **10** $\rightarrow$ **9** $\rightarrow$ **8**).

Table 5 Mulliken population analysis for the stable intermediates of H_2 on M9 model.

	$q_{Zn}/\|e\|$	$q_{H_A}/\|e\|$	$q_{H_B}/\|e\|$	$q_Z/\|e\|$
2	0.46	0.31	−0.05	−0.72
4	0.01	0.26	0.32	−0.59
6	0.33	−0.02	0.34	−0.65
9	0.48	0.32	−0.07	−0.78
10	0.05	0.29	0.35	−0.69
11	0.33	−0.02	0.33	−0.64

Calculation showed that localisation and coordination of the Zn cation have essential influence on the interaction of the cation with H_2. As far as hydrogen molecule does not interact with framework oxygen atoms, the higher coordination number implies the less positive zinc cation and the weaker hydrogen activation (Δr_{HH}). Moreover, even strong symmetric activation cannot lead to dissociation as easily as when the interaction with framework oxygen atoms is present.

The vibrational analysis allows for studying the influence of temperature on the rate constants of elementary steps. As can be derived from Fig. 9, the temperature raise destabilises the structures comprising/including the gas phase moieties. This is due to the dominant contribution of the translational and rotational entropy comparing to the frustrated rotations the translation and rotation degrees of freedom are converted to upon adsorption.

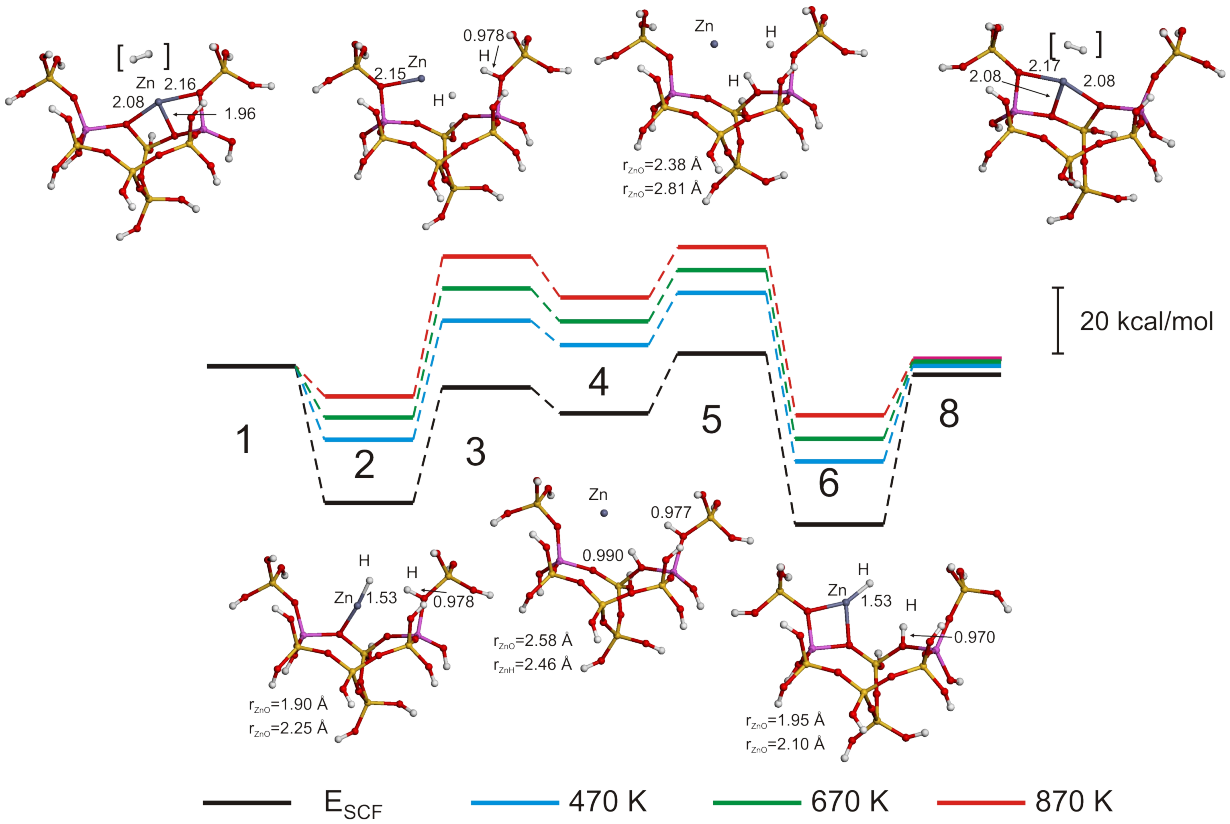

Fig. 9 Reaction path for hydrogen adsorption without (SCF energy, black) and with temperature correction at various temperatures (free energies as blue, green, and red lines), bond lengths are given in Å; part 1.

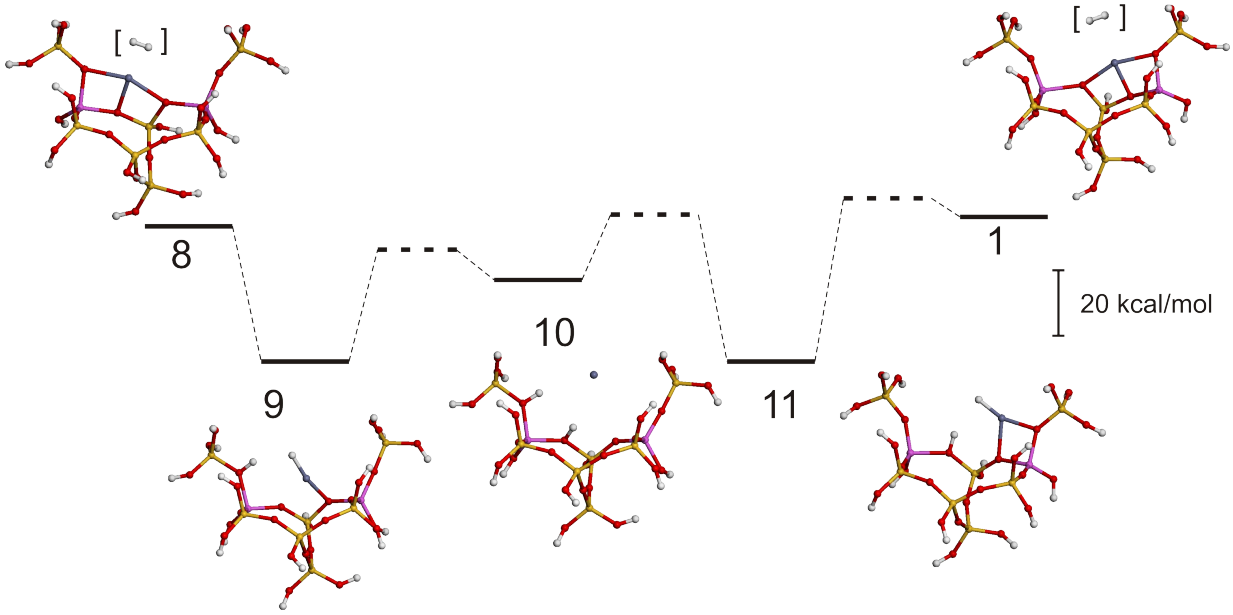

Fig. 10 Reaction path for hydrogen adsorption on active Zn site, part 2.

Conclusions

Depending on the cation and the surrounding framework the hydrogen activation can vary in a wide range – from only slight weakening of the H-H bond to utter dissociation of H_2 molecule. The results obtained for the interaction between H_2 and cations Ag^+, Cu^+ , Mg^{2+}, Cd^{2+}, Zn^{2+} in cluster model of several sizes indicate that there are three main factors determining hydrogen activation: σ-donation from σ_{H_2} to the cation, π-backdonation from the cation to antibonding $\sigma^*_{H_2}$ orbitals, and interaction between H_2 molecule and framework oxygen atoms. First two of them are described by orbital interaction and are, in general, characterized by orbital interaction energy, ΔE_{orb}, which includes the components of donation and backdonation processes depending strongly on the cation. For one group of cations, *e.g.* Ag^+ and Cu^+, the backdonation is more efficient, while for the others the σ-donation is privileged. These processes can be moderated by the surrounding zeolite framework, which hinders the σ-donation and enhances the π-backdonation. The coordination number of the cation correlates positively with the significance of the zeolite framework influence. The NOCV analysis allowed to elucidate the components for individual channels of the activation process and also to conclude that the backdonation is more efficient in weakening the H-H bond than the donation channels. The third factor of H-H activation is the distance between the approaching hydrogen molecule and framework oxygen atom combined with the charge accumulated on the molecule. It varies dramatically from one cation localisation to another; it is, however, important that the place stable for one cation is not necessarily stable for the other. Zinc cation can coordinate to zeolite framework in many conformations and the localisation of Zn^{2+} for which the H_2 molecule dissociates was identified. In other localisation, even more stable by $32-35$ kcal/mol, zinc site activates H-H bond only slightly ($\Delta\nu \approx -200$ cm^{-1}). Thus the geometry of the site, larger then the first coordination sphere, determines the ability of the site to activate (or even dissociate) adsorbed molecule. In the case of Zn-MFI the low coordination number of Zn^{2+} corresponds to the geometry which allows for the interaction of positively charged H_2 with framework oxygen atom and enhances the formation of OH group and $Z-O-(ZnH)^+$ cation. Based of the calculations, the mechanism of H_2 transformations has been proposed and it points out a possibility of an analogous C-H bond activation. Upon heterolytic dissociation the Zn^0 moiety can be formed together with two OH groups. Eventually, in two elementary steps the H_2 molecule can be restored.

Acknowledgement

The authors gratefully acknowledge Mrs Natalia Kubica for performing some computations as well as National Science Centre for the financial support (Grant No.: 2011/01/B/ST5/00915).

References

1 L. Wang, R. T. Yang, New sorbents for hydrogen storage by hydrogen spillover – a review, Energy & Environmental Science 1 (2) (2008) 268.

2 U. Eberle, M. Felderhoff, F. Schüth, Chemical and physical solutions for hydrogen storage., Angewandte Chemie (International ed. in English) 48 (36) (2009) 6608–30.

3 P. Jena, Materials for hydrogen storage: Past, present, and future, The Journal of Physical Chemistry Letters 2 (3) (2011) 206–211.

4 E. Broclawik, J. Datka, B. Gil, P. Kozyra, Why Cu^+ in ZSM-5 framework is active in DeNOx reaction – quantum chemical calculations and IR studies, Catalysis Today 75 (2002) 353–357.

5 J. Datka, E. Kukulska-Zając, W. Kobyzewa, The activation of acetylene by Cu^+ ions in zeolites studied by IR spectroscopy, Catalysis Today 101 (2005) 123–129.

6 J. Datka, E. Kukulska-Zając, P. Kozyra, IR and TPD studies of the interaction of alkenes with Cu^+ sites in CuNaY and CuNaX zeolites of various Cu content. The heterogeneity of Cu^+ sites, Journal of Molecular Structure 794 (1-3) (2006) 261–264.

7 E. Broclawik, P. Rejmak, P. Kozyra, J. Datka, DFT quantum chemical modeling of the interaction of alkenes with Cu^+ sites in zeolites, Catalysis Today 114 (2-3) (2006) 162–168.

8 E. Broclawik, J. Załucka, P. Kozyra, M. Mitoraj, J. Datka, New insights into charge flow processes and their impact on the activation of ethene and ethyne by Cu(I) and Ag(I) sites in MFI, The Journal of Physical Chemistry C 114 (21) (2010) 9808–9816.

9 E. Broclawik, J. Załucka, P. Kozyra, M. Mitoraj, J. Datka, Formaldehyde activation by Cu(I) and Ag(I) sites in ZSM-5: ETS-NOCV analysis of charge transfer processes, Catalysis Today 169 (1) (2011) 45–51.

10 P. Kozyra, J. Załucka, M. Mitoraj, E. Brocławik, J. Datka, From electron density flow towards activation: Benzene interacting with Cu(I) and Ag(I) sites in ZSM-5. DFT modeling, Catalysis Letters 126 (3-4) (2008) 241–246.

11 P. Kozyra, E. Broclawik, M. Mitoraj, J. Datka, C≡C, C=C, and C=O bond activation by coinage metal cations in ZSM-5 zeolites: Quantitative charge transfer resolution, The Journal of Physical Chemistry C 117 (15) (2013) 7511–7518.

12 P. Kozyra, W. Piskorz, Spin-resolved NOCV analysis of the zeolite framework influence on the interaction of NO with Cu(I/II) sites in zeolites., Physical Chemistry Chemical Physics 17 (20) (2015) 13267–73.

13 A. G. Stepanov, S. S. Arzumanov, A. A. Gabrienko, V. N. Parmon, I. I. Ivanova, D. Freude, Significant influence of Zn on activation of the C-H bonds of small alkanes by Brønsted acid sites of zeolite, ChemPhysChem 9 (17) (2008) 2559–2563.

14 A. Smiešková, E. Rojasová, P. Hudec, L. Šabo, Aromatization of light alkanes over ZSM-5 catalysts influence of the particle properties of the zeolite, Applied Catalysis A: General 268 (2004) 235–240.

15 J. A. Biscardi, G. D. Meitzner, E. Iglesia, Structure and density of active Zn species in Zn/H-ZSM5 propane aromatization catalysts, Journal of Catalysis 179 (1) (1998) 192–202.

16 V. B. Kazansky, V. Y. Borovkov, A. I. Serikh, R. A. v. Santen, B. G. Anderson, Nature of the sites of dissociative adsorption of dihydrogen and light paraffins in ZnHZSM-5 zeolite prepared by incipient wetness impregnation, Catalysis Letters 66 (1-2) (2000) 39–47.

17 V. B. Kazansky, DRIFT study of molecular and dissociative adsorption of light paraffins by HZSM-5 zeolite modified with zinc ions: methane adsorption, Journal of Catalysis 225 (2004) 369–373.

18 X. Wang, J. Xu, G. Qi, B. Li, C. Wang, F. Deng, Alkylation of benzene with methane over ZnZSM-5 zeolites studied with solid-state NMR spectroscopy, The Journal of Physical Chemistry C 117 (2013) 4018–4023.

19 B. Civalleri, F. J. Torres, R. Demichelis, A. Terentyev, P. Ugliengo, Ab initio investigation of the interaction of H_2 with lithium exchanged low-silica chabazites, Journal of Physics: Conference Series 117 (2008) 012012.

20 L. Kang, W. Deng, K. Han, T. Zhang, Z. Liu, A DFT study of adsorption hydrogen on the Li-FAU zeolite, International Journal of Hydrogen Energy 33 (1) (2008) 105–110.

21 M. F. Fellah, Hydrogen adsorption on M-ZSM-12 zeolite clusters (M = K, Na and Li): a density functional theory study, Journal of Porous Materials 21 (5) (2014) 883–888.

22 P. Nachtigall, E. Garrone, G. T. Palomino, M. R. Delgado, D. Nachtigallová, C. O. Areán, FTIR spectroscopic and computational studies on hydrogen adsorption on the zeolite Li-FER, Physical Chemistry Chemical Physics: PCCP 8 (19) (2006) 2286–92.

23 F. J. Torres, J. G. Vitillo, B. Civalleri, G. Ricchiardi, Interaction of H_2 with alkali-metal-exchanged zeolites: a quantum mechanical study, The Journal of Physical Chemistry C 111 (99 590) (2007) 2505–2513.

24 F. J. Torres, B. Civalleri, A. Terentyev, P. Ugliengo, C. Pisani, Theoretical study of molecular hydrogen adsorption in Mg-exchanged chabazite, Journal of Physical Chemistry C 111 (5) (2007) 1871–1873.

25 C. O. Areán, G. T. Palomino, M. R. L. Carayol, A. Pulido, M. Rubeš, Hydrogen adsorption on the zeolite Ca-A: DFT and FT-IR investigation, Chemical Physics Letters 477 (2009) 139–143.

26 X. Solans-Monfort, M. Sodupe, C. M. Zicovich-Wilson, E. Gribov, G. Spoto, C. Busco, P. Ugliengo, Can Cu^+-exchanged zeolites store molecular hydrogen? An ab-initio periodic study compared with low-temperature FTIR, The Journal of Physical Chemistry B 108 (24) (2004) 8278–8286.

27 F. J. Torres, P. Ugliengo, B. Civalleri, A. Terentyev, C. Pisani, A review of the computational studies of proton- and metal-exchanged chabazites as media for molecular hydrogen storage performed with the CRYSTAL code, International Journal of Hydrogen Energy 33 (2) (2008) 746–754.

28 X. Solans-Monfort, M. Sodupe, J. Eckert, Origin of the enhanced interaction of molecular hydrogen with extraframework Cu^+ and FeO^+ cations in zeolite hosts. A periodic DFT study, The Journal of Physical Chemistry C 114 (32) (2010) 13926–13934.

29 G. Yang, L. Zhou, X. Liu, X. Han, X. Bao, Adsorption, reduction and storage of hydrogen within ZSM-5 zeolite exchanged with various ions: A comparative theoretical study, Microporous and Mesoporous Materials 161 (2012) 168–178.

30 V. B. Kazansky, A. Serykh, A new charge alternating model of localization of bivalent cations in high silica zeolites with distantly placed aluminum atoms in the framework, Microporous and Mesoporous Materials 70 (1-3) (2004) 151–154.

31 V. B. Kazansky, A. I. Serykh, Unusual forms of molecular hydrogen adsorption by Cu^{+1} ions in the copper-modified ZSM-5 zeolite, Catal. Lett. 98 (2004) 77–79.

32 V. B. Kazansky, E. A. Pidko, A new insight in the unusual adsorption properties of Cu^+ cations in Cu-ZSM-5 zeolite, Catalysis Today 110 (3-4) (2005) 281–293.

33 Y. G. Kolyagin, V. V. Ordomsky, Y. Khimyak, A. K. Rebrov, F. Fajula, I. I. Ivanova, Initial stages of propane activation over Zn/MFI catalyst studied by in situ NMR and IR spectroscopic techniques, Journal of Catalysis 238 (1) (2006) 122–133.

34 Y. G. Kolyagin, I. I. Ivanova, V. V. Ordomsky, A. Gedeon, Y. A. Pirogov, Methane activation over Zn-modified MFI zeolite: NMR evidence for Zn-methyl surface species formation, The Journal of Physical Chemistry C 112 (2008) 20065–20069.

35 A. Oda, H. Torigoe, A. Itadani, T. Ohkubo, T. Yumura, H. Kobayashi, Y. Kuroda, Mechanism of CH_4 activation on a monomeric Zn^{2+}-ion exchanged in MFI-type zeolite with a specific Al arrangement: Similarity to the activation site for H_2, Journal of Physical Chemistry C 117 (38) (2013) 19525–19534.

36 A. Oda, H. Torigoe, A. Itadani, T. Ohkubo, T. Yumura, H. Kobayashi, Y. Kuroda, An important factor in CH_4 activation by Zn ion in comparison with Mg ion in MFI: The superior electron-accepting nature of Zn^{2+}, Journal of Physical Chemistry C 118 (28) (2014) 15234–15241.

37 L. Benco, T. Bucko, J. Hafner, H. Toulhoat, A Density Functional Theory study of molecular and dissociative adsorption of H_2 on active sites in mordenite, Journal of Physical Chemistry B 109 (2005) 22491–22501.

38 L. A. M. M. Barbosa, R. A. van Santen, Study of the activation of C-H and H-H chemical bonds by the $[ZnOZn]^{2+}$ oxycation: Influence of the zeolite framework geometry, Journal of Physical Chemistry B 107 (51) (2003) 14342–14349.

39 L. A. M. M. Barbosa, R. A. van Santen, The Activation of H_2 by Zeolitic Zn(II) Cations, Journal of Physical Chemistry C 111 (23) (2007) 8337–8348.

40 V. B. Kazansky, State and properties of ion-exchanged cations in zeolites: 1. IR spectra and chemical activation of adsorbed molecular hydrogen, Kinetics and Catalysis 55 (4) (2014) 492–501.

41 V. B. Kazansky, A. I. Serykh, B. G. Anderson, R. A. van Santen, The Sites of Molecular and Dissociative Hydrogen Adsorption in High-Silica Zeolites Modified with Zinc Ions. III DRIFT Study of H2 Adsorption by the Zeolites with Different Zinc Content and Si/Al Ratios in the Framework, Catalysis Letters 88 (3-4) (2003) 211–217.

42 A. A. Shubin, G. M. Zhidomirov, V. B. Kazansky, R. A. van Santen, DFT cluster modeling of molecular and dissociative hydrogen adsorption on Zn^{2+} ions with distant placing of aluminum in the framework of high-silica zeolites, Catal. Lett. 90 (2003) 137–142.

43 A. Oda, H. Torigoe, A. Itadani, T. Ohkubo, T. Yumura, H. Kobayashi, Y. Kuroda, Unprecedented reversible redox process in the ZnMFI-H_2 system involving formation of stable atomic Zn(0), Angew. Chem. Int. Ed. 51 (31) (2012) 7719–23.

44 R. Ahlrichs, M. Bär, M. Häser, H. Horn, C. Kölmel, Electronic structure calculations on workstation computers: The program

system Tturbomole, Chemical Physics Letters 162 (3) (1989) 165–169.
45 R. C. Lochan, M. Head-Gordon, Computational studies of molecular hydrogen binding affinities: the role of dispersion forces, electrostatics, and orbital interactions, Physical Chemistry Chemical Physics 8 (12) (2006) 1357–70.
46 S. Grimme, Semiempirical GGA-type density functional constructed with a long-range dispersion correction, Journal of Computational Chemistry 27 (15) (2006) 1787–1799.
47 M. Mitoraj, A. Michalak, Natural orbitals for chemical valence as descriptors of chemical bonding in transition metal complexes, Journal of Molecular Modeling 13 (2) (2007) 347–355.
48 M. Mitoraj, A. Michalak, Donor-acceptor properties of ligands from the natural orbitals for chemical valence, Organometallics 26 (26) (2007) 6576–6580.
49 A. Michalak, M. Mitoraj, T. Ziegler, Bond orbitals from chemical valence theory, J. Phys. Chem. A 112 (9) (2008) 1933–9.
50 M. Radoń, On the properties of natural orbitals for chemical valence, Theor. Chem. Account 120 (2008) 337–339.
51 T. Ziegler, A. Rauk, A theoretical study of the ethylene-metal bond in complexes between Cu^+, Ag^+, Au^+, Pt^0, or Pt^{2+} and ethylene, based on the Hartree-Fock-Slater transition-state method, Inorg. Chem. 18 (6) (1979) 1558–1565.
52 J. Sauer, M. Sierka, Combining quantum mechanics and interatomic potential functions in *ab initio* studies of extended systems, Comp. Chem. 21 (2000) 1470.
53 C. Tuma, J. Sauer, A hybrid MP2/planewave-DFT scheme for large chemical systems: proton jumps in zeolites, Chem. Phys. Lett. 387 (2004) 388.
54 D. R. Lide (Ed.), CRC Handbook of Chemistry and Physics, 89th Edition, CRC Press: Taylor and Francis, Boca Raton, FL, 2009.
55 C. Lamberti, A. Zecchina, E. Groppo, S. Bordiga, Probing the surfaces of heterogeneous catalysts by in situ IR spectroscopy, Chemical Society Reviews 39 (12) (2010) 4951–5001.
56 G. Spoto, E. Gribov, S. Bordiga, C. Lamberti, G. Ricchiardi, $Cu^+(H_2)$ and $Na^+(H_2)$ adducts in exchanged ZSM-5 zeolites, Chem. Commun. (2004) 2768–2769.
57 A. I. Serykh, Unusually strong adsorption of molecular hydrogen on Cu^+ sites in copper-modified ZSM-5, Phys. Chem. Chem. Phys. 6 (2004) 5250–5255.
58 G. Berlier, E. Gribov, D. Cocina, G. Spoto, A. Zecchina, Probing the Brønsted and Lewis acidity of Fe-silicalite by FTIR spectroscopy of H_2 adsorbed at 20 K: Evidences for the formation of Fe^{3+}/H_2 and Fe^{2+}/H_2 molecular adducts, Journal of Catalysis 238 (2) (2006) 243–249.

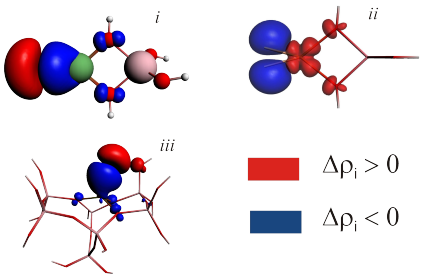

Abstract

Three essential factors have been identified (*i*-*iii*) for the interaction between H_2 and Ag^+, Cu^+, Mg^{2+}, Cd^{2+}, and Zn^{2+} sites in zeolites. In the case of bare cation the main contribution is a donation from σ_{H_2} to the cation (*i*). When zeolite framework surrounding the cation is introduced, it hinders σ-donation and enhances π-backdonation from the cation to antibonding orbital of the molecule (*ii*). For the Zn^{2+} position for which H_2 molecule dissociates, the interaction between H_2 and oxygen framework (*iii*) plays crucial role. Based on the calculations the mechanism of H_2 transformations has been proposed.